

FDG PET IN THE MANAGEMENT OF LUNG CANCER

Kevin KM Tse, MD, Helene Reich, MD, Jane Alavi, MD, and
Abass Alavi, MD

Division of Nuclear Medicine, Department of Radiology and Division of Oncology,
Department of Medicine, Hospital of the University of Pennsylvania, PA, USA

ABSTRACT

We describe a patient with newly diagnosed lung cancer. Staging was performed with CT and mediastinoscopy. FDG PET scan was performed and confirmed increased metabolic activity in the primary tumor as well as the hilar lymph node. Seven months after initial presentation, the patient was found to have two lytic lesions in the pelvis on plain radiograph. Bone scan was negative but PET demonstrated FDG uptake in one lesion. The possible utility of whole body FDG PET in detecting osseous metastasis is discussed. The state-of-the-art of staging lung cancer is also reviewed.

Key words: FDG; PET; lung cancer; staging; metastasis

CASE SUMMARY

A 72-year-old male presented to the Hospital of the University of Pennsylvania in January, 1993 for intermittent coughing spells. He first noticed a productive cough in September, 1992. At that time, he had a low grade fever and was treated with antibiotics. He noticed some improvement, with resolution of his fever. However, he continued to have a cough productive of whitish sputum. A chest radiograph in early January demonstrated opacification on the right upper lobe with associated volume loss (Fig. 1).

The patient was a chronic smoker with a 40 pack-year history of tobacco use. He denied any shortness of breath, decrease in exercise tolerance or weight loss. On physical examination, he was a healthy appearing white male in no acute distress. Lymphadenopathy was not detected. Auscultation of the chest revealed bronchial breath sounds in the right upper chest. Air entry was good bilaterally and no wheezes or crackles were detected. Cardiac examination was normal. Abdominal and neurological examina-

tions were normal. Clubbing was not identified.

Bronchoscopy demonstrated an endobronchial lesion. Histology and cytology revealed moderately differentiated squamous cell carcinoma. A metastatic workup included a normal computed tomographic (CT) scan of the head. CT of the chest showed right upper lobe collapse with mass effect, cavitation, and necrosis, consistent with an obstructing tumor (Fig. 2). A right pleural-based mass was also found and thought to be consistent with tumor. Anterior and precarinal lymphadenopathy was detected as well as an 8 mm nodule in the peripheral left upper lung. In addition, there was irregularity of the right costovertebral junction at T-7 which was suspicious for tumor involvement (Fig. 3). Both adrenal glands were unremarkable. A total body bone scan demonstrated areas of increased uptake at the right 7th costovertebral junction and the left anterior 4th rib (Fig. 4). Plain radiographs of the ribs were normal.

Positron emission tomography (PET) scan of the chest using fluorine-18 deoxyglucose (FDG) demonstrated significant uptake in the right

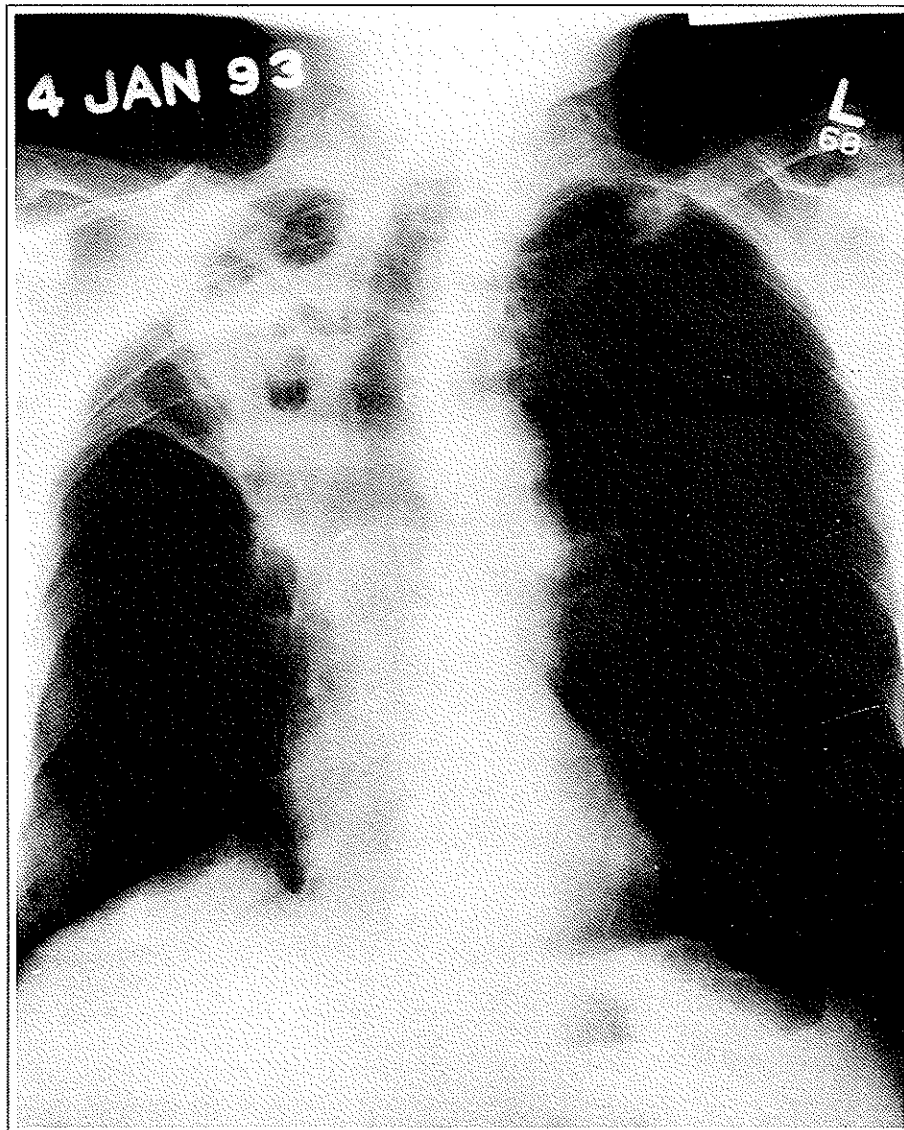


Fig. 1. Chest radiograph demonstrates opacification of the right upper lobe with associated volume loss.

upper lobe and the right pleural-based tumor (Fig. 5). In addition, significant uptake was present in the right hilum which was interpreted to be consistent with lymph node involvement (Fig. 6). No abnormal uptake was detected at the right 7th costovertebral junction.

Subsequently, the patient underwent mediastinoscopy. Biopsy of a right paratracheal mass at level 2 was found to be positive for squamous cell carcinoma. Therefore, he was staged as T2N2, IIIA. He was treated with radiation therapy and chemotherapy including VP-16 and cisplatin. A follow-up CT of the chest showed a

decrease in size in both the precarinal adenopathy and right upper lobe tumor. Bone scan after treatment showed no new lesions with a stable appearance of the previously identified lesions. He was stable until July, 1993 when he started to experience some pain in the right hip. A radiograph of the right hip showed two lucent areas in the right ilium and the ischium close to the acetabulum (Fig. 7). However, the bone scan on July 22, 1993 demonstrated no abnormal uptake in the right pelvis (Fig. 8). A second total body PET scan with FDG was performed on July 21, 1993. This demonstrated a single focus of

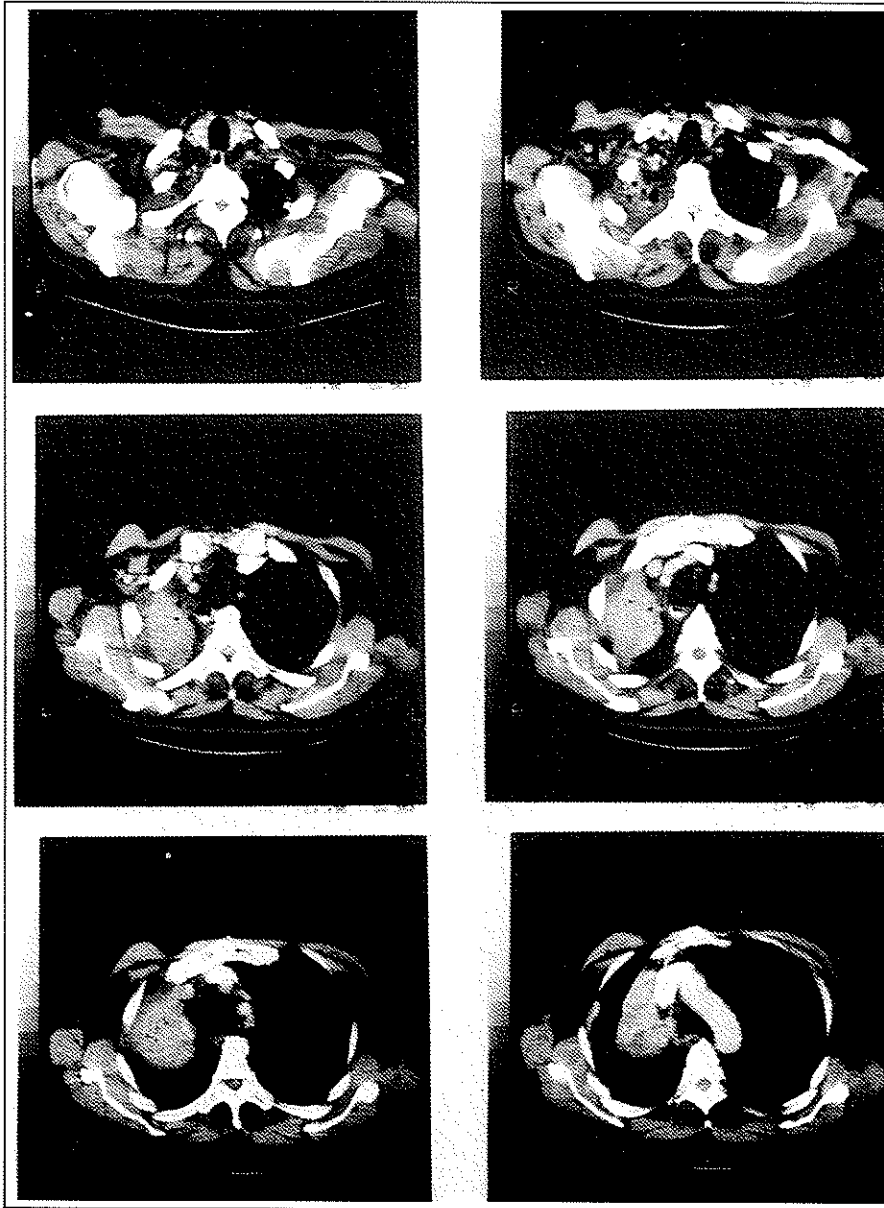


Fig. 2. Contrast-enhanced chest CT demonstrates a mass in the right upper lobe with areas of cavitation and areas of relatively lower density suggesting necrosis. There is associated volume loss.

intense uptake in the right ilium which is consistent with bony metastasis, and no significant uptake was seen in the thorax (Fig. 9).

DISCUSSION

Background

Primary lung cancer is the most common malignancy seen in the United States and

continues to have a very high mortality because of late diagnosis and ineffectiveness of therapy. In 1992, lung cancer accounted for about 28% of all cancer-related deaths. The 5-year survival rate is only 13% overall (1).

Most lung cancers are not diagnosed until the patient presents with symptoms. Unfortunately, by the time the lung cancer is clinically overt, it is usually at a more advanced stage. The main reason for late diagnosis is the lack of effective

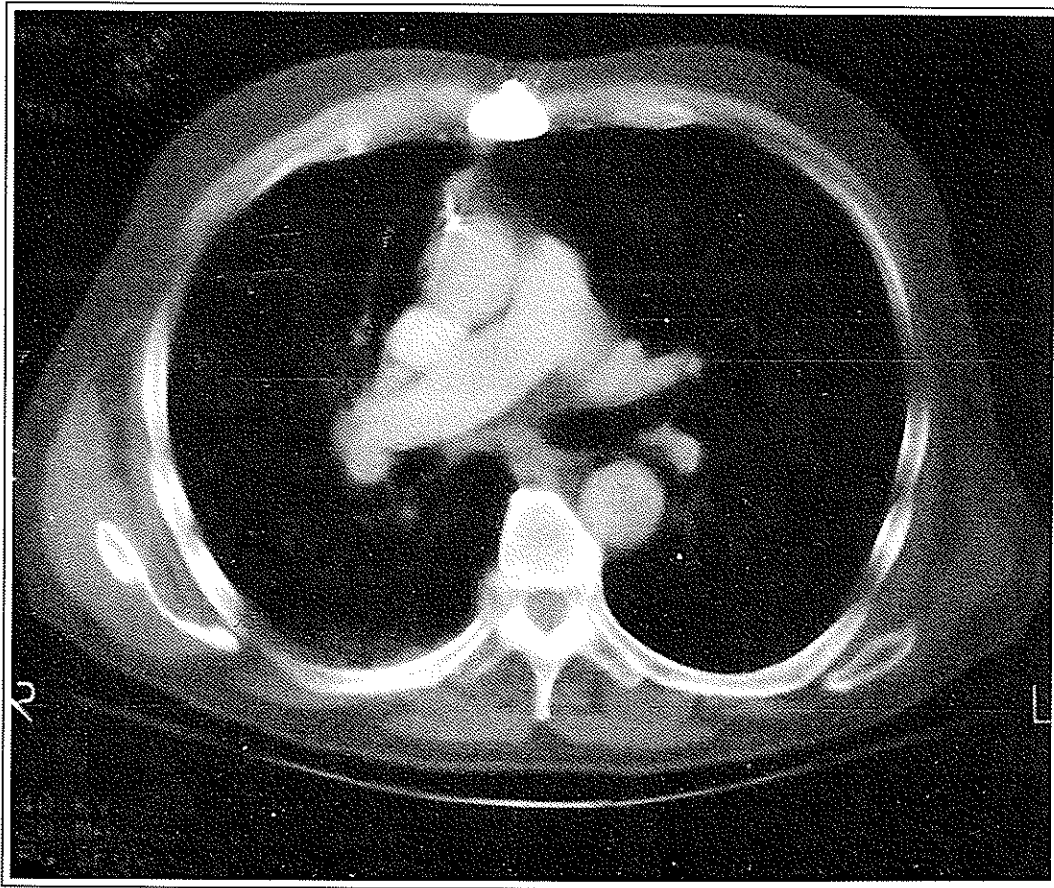


Fig. 3. Chest CT at the level of the right pulmonary artery demonstrates a soft tissue density mass in the right costovertebral junction.

screening techniques. Screening with chest radiographs and sputum cytology have failed to show any improvement in survival (2-4). As a result, the American Cancer Society, as of 1980, has recommended against the use of chest radiographs and sputum cytology as screening tools (5).

In recent years, surgeons have performed more aggressive resections, and adjuvant chemotherapy and radiation therapy for borderline operable or inoperable cases hoping that this aggressive approach may provide longer disease free intervals (6-10). With the increasing availability of aggressive treatments, it becomes very important to stage these patients as accurately as possible. Precise staging guides clinicians in the proper grouping of patients with regard to prognosis and treatment regimens. Progress in imaging technology such as CT, MRI and PET allows for far greater accuracy in tumor staging and monitoring of therapy. The ideal

imaging technique should be able to distinguish metastatic from uninvolved lymph nodes, localize the optimal sites for biopsy, identify which patients would benefit from aggressive surgery, determine whether an adrenal mass should be biopsied, and differentiate recurrent tumor from therapy-induced changes. Other invasive staging procedures include bronchoscopy, percutaneous needle biopsy, mediastinoscopy, and thoracoscopy including video-assisted thoracoscopic surgery.

Staging with CT and MRI

The superior spatial resolution of CT permits a detailed assessment of lung parenchyma and airways. It is also helpful in identifying mediastinal adenopathy in many patients. There are significant limitations to this technique, however. Because CT is a transaxial technique, areas with a vertical orientation including the aortopulmonary window, subcarinal region,

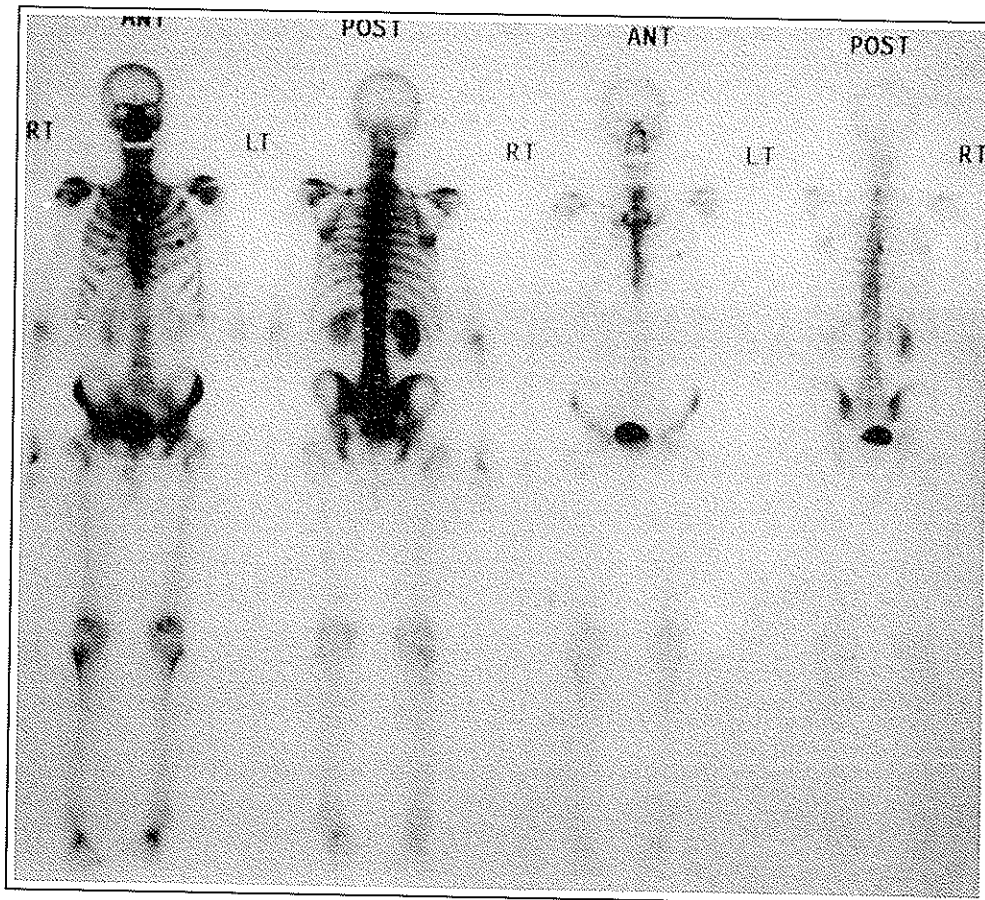


Fig. 4. Total body scan demonstrates focal increased activity in the right 7th costovertebral junction and in the left anterior 4th rib.

thoracocervical junction, and peridiaphragmatic region may be difficult to assess. The introduction of MRI has a definite impact on improving some of the shortcomings of CT. The multiplanar capability of MRI is an obvious advantage over CT. MRI has better contrast resolution when compared to CT, but its poorer spatial resolution may limit this advantage. Vascular structures can be visualized by MRI without the requirement of intravenous contrast material. Evaluation of lung parenchyma, however, is hampered by the low intrinsic signal of parenchymal structures, relatively poor spatial resolution and image degradation due to respiratory motion.

The diagnosis of nodal metastasis on CT relies exclusively on the demonstration of nodal enlargement. The size above which a node should be considered abnormal remains highly controversial. It is known that lymph nodes of

normal size may actually contain micro-metastases. On the other hand, enlarged nodes may be due to an inflammatory process and contain no malignant tissue at all. In a recent study by Mcloud et al, 37% of lymph nodes measuring 2 to 4 cm in diameter on CT did not contain metastases (11). There is a wide range of value in the literature for the sensitivity and specificity of CT in the evaluation of mediastinal lymphadenopathy. The reported sensitivity ranges from 24 to 95%, and the specificity varies from 23 to 100% (11-24). Many of these studies suffered from lack of a standard size criterion for lymph nodes. MRI is not able to differentiate hyperplastic from metastatic lymph nodes in the mediastinum and hilum based on imaging parameters (25). The accuracy of MRI in detecting mediastinal and hilar lymphadenopathy is comparable to that of CT (26).

The evaluation of chest wall involvement by

lung cancer using CT has been disappointing. Criteria postulated in the evaluation of chest wall involvement include an obtuse angle of the tumor with the pleura, more than 3 cm of tumor contact with the pleura, pleural thickening, the presence of a chest wall soft tissue mass, and rib destruction. Pearlberg et al found that definite

bony destruction was the only reliable finding of chest wall invasion on CT (27). Chest wall invasion is better demonstrated by MRI due to the high soft tissue contrast between tumor and muscle, however, direct comparison of MRI with CT has failed to show a definite advantage for either one (28,29).

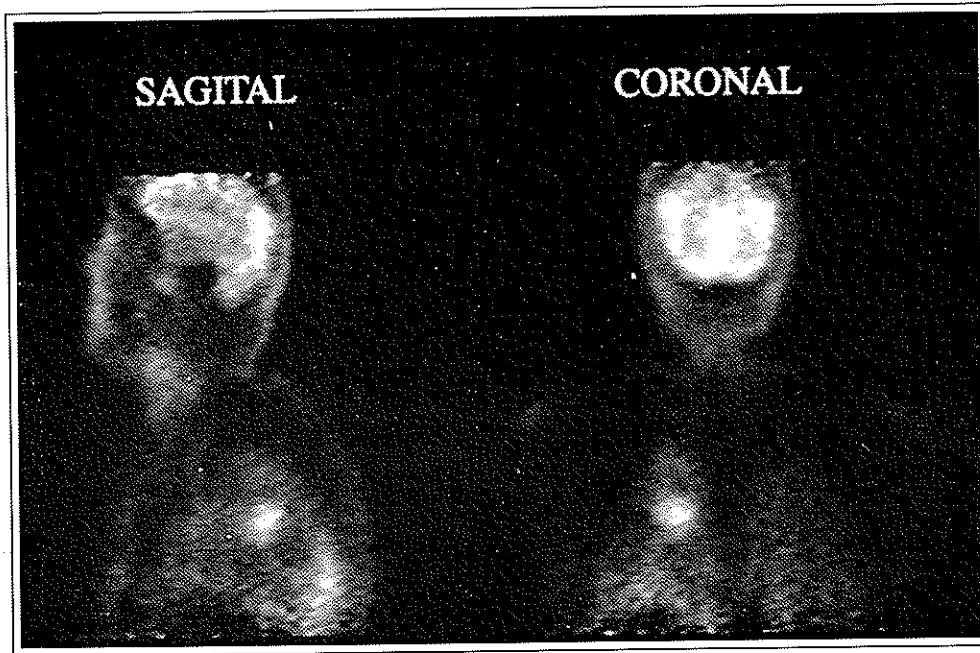


Fig. 5. FDG PET scan of the head and chest demonstrates a focus of increased activity in the right upper lobe and posteriorly along the pleura on the right.

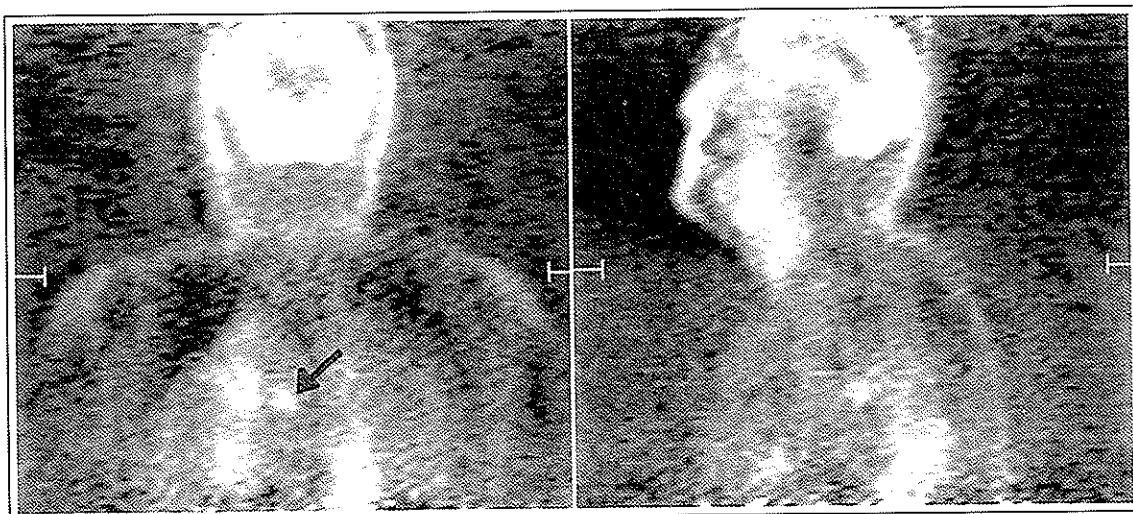


Fig. 6. FDG PET scan demonstrates the right hilar lesion (arrow) as well as the primary tumor in the right upper lobe.

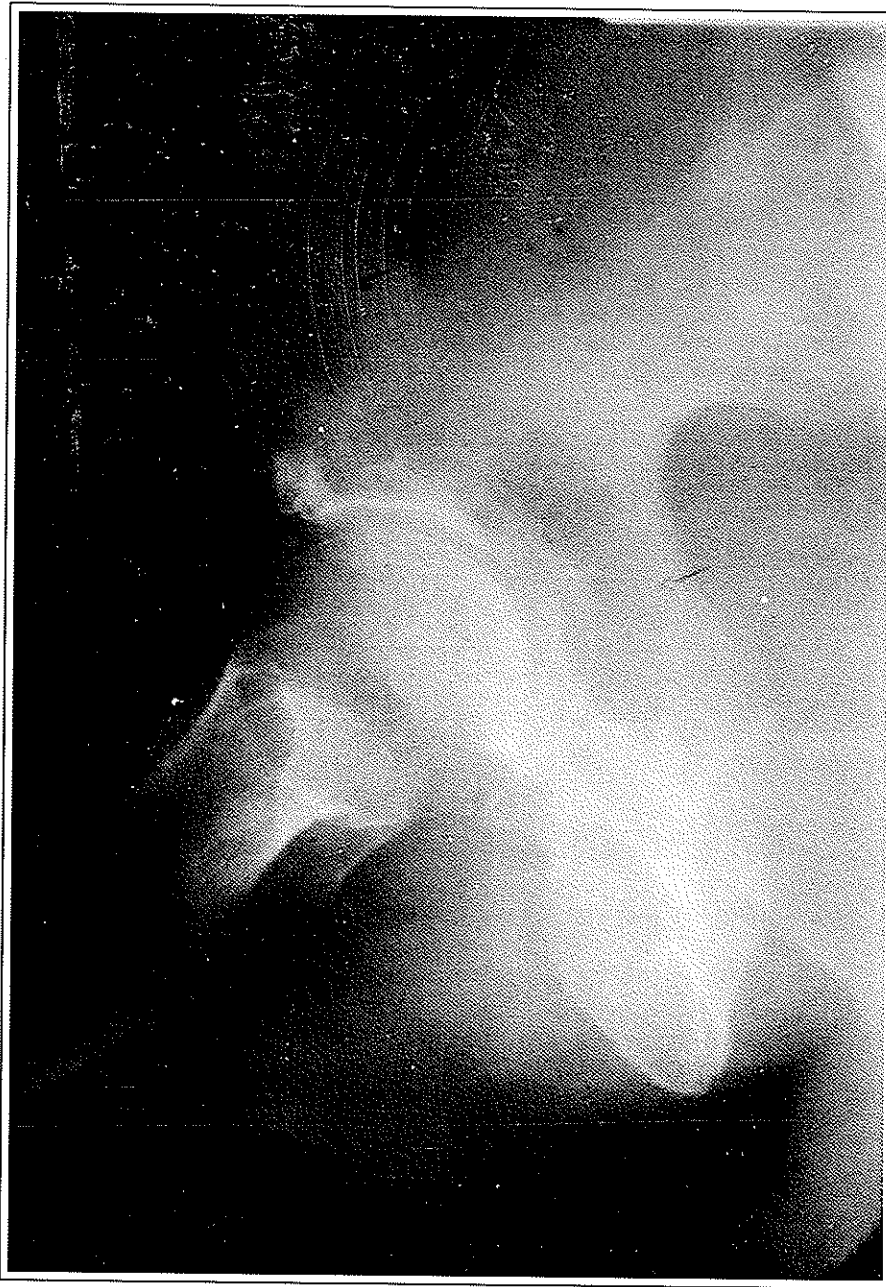


Fig. 7. Right hip radiograph demonstrates lucencies in the right ilium and right ischium.

CT is also not very effective in the evaluation of mediastinal invasion by lung cancer. The reported sensitivity and specificity is only about 70% (13). Superior sulcus or Pancoast tumor is another area that is not easily assessed by CT. Anatomy in this area is better demonstrated on coronal and sagittal images. Heelan et al have shown that MRI is more sensitive than CT in

identifying tumor invasion through the superior sulcus of the lung (30).

Another area of difficulty in staging these patients is determining the etiology of adrenal masses which are frequently discovered on CT. More than two thirds of these lesions prove to represent benign adenomas (31). CT and MRI have not been reliable in identifying the origin of

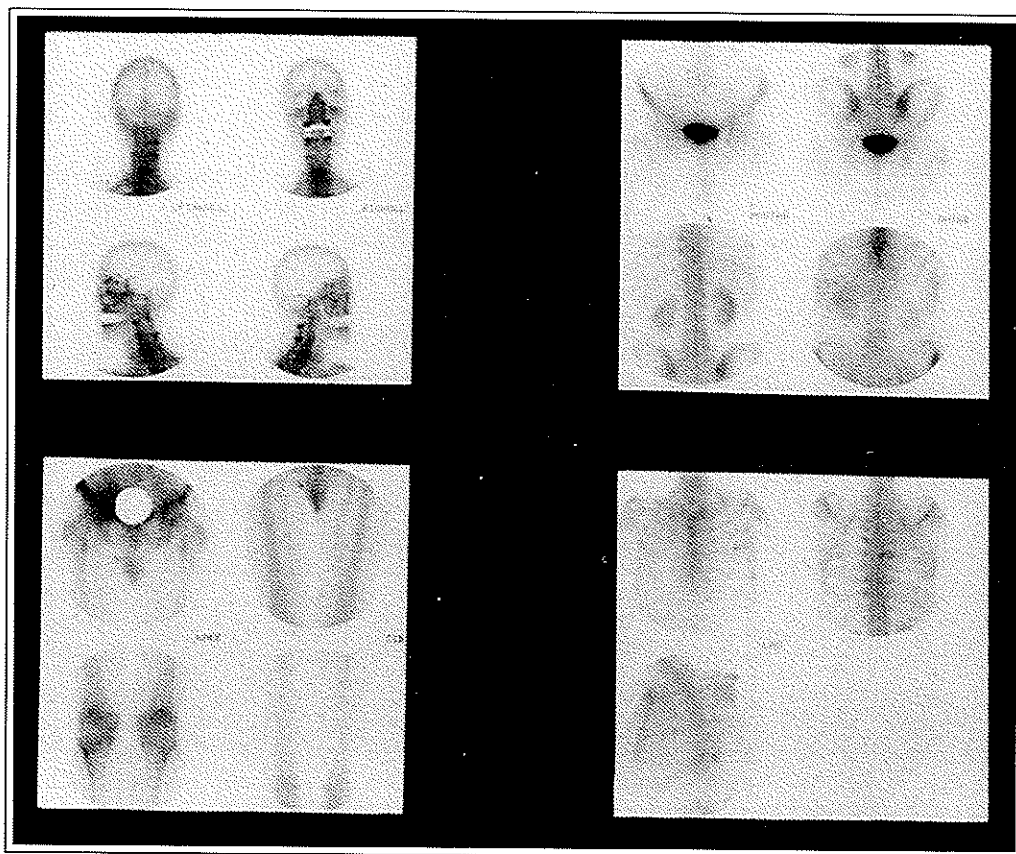


Fig. 8. Total body bone scan demonstrates no abnormal uptake in the right plevis. Again noted is increased uptake in the right 7th costovertebral junction and the left 4th anterior rib.

adrenal masses. CT can differentiate adenomas from malignant lesions in only 52% of cases (32). On T2 weighted MRI images, adrenal adenomas have low signal intensity, whereas metastases usually have higher signal intensity (33,34). Unfortunately, the signal intensity ratio is not able to differentiate benign from malignant adrenal masses in as many as 30% of cases (26). It is frequently necessary to attempt needle biopsy or surgical biopsy of an adrenal mass in order to determine if the patient has operable or metastatic lung cancer.

In addition, after surgery or radiation therapy, there is often considerable fibrosis and distortion of the normal anatomy in the mediastinum or lung, making interpretation of chest radiographs or CT scans very difficult. Streak artifacts from surgical clips can be troublesome as well. MRI may prove to be more useful than CT in this setting (35). Recurrent tumor has high signal intensity on T2 weighted images, whereas mature fibrosis has low signal intensity. Radiation

induced pneumonitis, immature fibrosis, and other inflammatory tissues, however, also produce high signal intensity on T2 weighted images. Confusion may arise in these situations (36).

FDG-PET in lung cancer

As we have discussed, both CT and MRI have limitations in the evaluation of primary tumor, nodal involvement and metastasis in lung cancer. An imaging modality that is capable of differentiating benign from malignant pulmonary lesions, define the extent of local and regional involvement, and evaluate metastasis would be helpful in patients with lung cancer. PET FDG is a unique imaging technique that allows us to measure metabolism in normal and diseased tissues and therefore offers a new approach to imaging disease activity. In 1930, Warburg et al found a higher rate of glycolysis (aerobic and anaerobic) in malignant tumors (37). The increased glycolysis in tumor cells has been

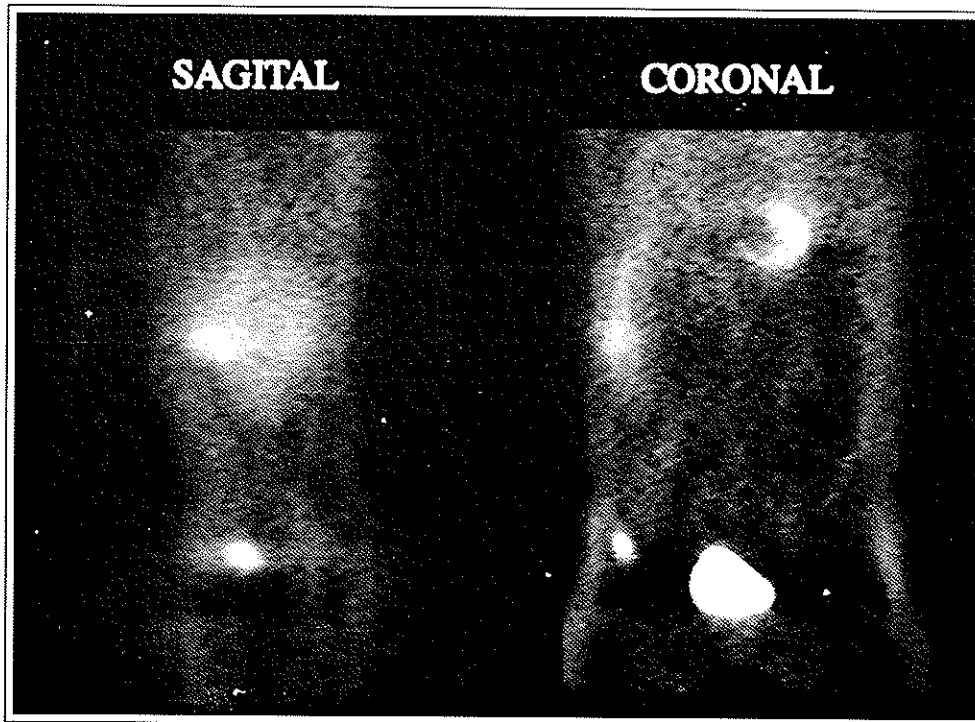


Fig. 9. FDG PET scan shows increased activity in the right ilium, corresponding to the hip radiograph.

linked to increased activity of glycolytic enzymes and increased membrane glucose transfer capability (38,39). As a glucose analog, FDG has been used as a PET radiopharmaceutical to image glucose metabolism. The first oncologic application of FDG in PET was in brain tumors (40,41). We and others have also shown that higher rates of glycolysis correlate with higher histological grades and a worse prognosis (42,43). A variety of different tumors that includes brain, head and neck, lung, breast, colon, soft tissue and bone have been evaluated with PET FDG in clinical trials (43-54).

In a prospective study of radiographically indeterminate solitary pulmonary nodules, PET FDG imaging was found to be highly accurate in detecting malignancy. In addition, none of the benign nodules demonstrated increased FDG uptake. The differential uptake ratio (a semi-quantitative uptake index normalized to the patient's weight and injected dose) also revealed a statistically significant difference between malignant and benign nodules (45,54). Knopp et al also found that PET FDG imaging is superior to CT examinations in characterizing mediastinal involvement (47). Kubota et al reported a sensitivity of 83% and specificity of 90% for

FDG in the evaluation of lung tumors (46). In our patient, the initial FDG PET scan demonstrated increased metabolic activity in the primary tumor and the right hilum. This supported the suspicion of the malignant nature of the hilar lymph node reported on CT scan. Both lesions were subsequently proven to be malignant by histology.

In the evaluation of tumor recurrence and response following therapy, PET may complement CT and MRI. In a study to investigate the ability of FDG PET in classifying thoracic lesions as benign or recurrent disease in 22 patients with previous thoracic malignancy, Knopp et al found that PET agreed with the final diagnosis in all patients, whereas 23% false positives and 27% false negatives were reported with CT (47). Similar results were also obtained by Gupta et al (48). In our patient, no significant FDG uptake was present in the thorax on the follow-up FDG PET scan. This is consistent with treatment-induced remission of the lung tumor and adenopathy.

Bone scintigraphy has been the method of choice for detection of bony metastasis and has been proven to be more sensitive than plain radiograph. The application of FDG PET in

assessing bony metastasis has not been fully explored. Sasaki et al reported two cases of bone tumors with high FDG uptake and negative uptake on a bone scan (58). Adler et al demonstrated a strong relationship between FDG uptake and grade of malignancy among musculoskeletal tumors (59).

In our patient, the initial bone scan showed a suspicious lesion at the right 7th costovertebral junction. However, no focal increased FDG uptake was detected on PET. Follow-up bone scan 7 months later demonstrated no progression in this lesion. Although biopsy was not performed in this lesion, this clearly illustrated the capability of FDG PET to differentiate malignant from benign bony lesion or low grade from high grade malignancy in bone. In addition, 2 lytic lesions were detected in the pelvis on plain radiograph of our patient which are negative on bone scan. We postulated that the lesion in the right ilium was so aggressive that no significant bony repair could be detected by bone scan, but the active metabolism in bony metastasis could easily be identified by FDG PET scan. The possible explanation for the inability to detect the second bony lesion in the right acetabulum will be discussed in the next paragraph.

PET imaging is not without limitations. The

main problem of the technique is its limited spatial resolution. Important clinical issues such as identifying tumor invasion of vascular structures, extrapleural invasion, and involvement of specific lymph nodes are beyond the capability of current PET technology. Normal myocardial uptake of FDG may also obscure interpretation in regions adjacent to the heart. Although fasting can minimize FDG uptake by the myocardium, Choi et al reported that significant myocardial uptake may occur in 60% of human subjects even after 16 hours of fasting (55). In whole body PET scans, intense bladder activity may also be a problem (Fig. 10). Assessment of some pelvic lesions become very difficult. In our patient, only one focus was identified in the right ilium on the follow-up FDG PET study and the lesion near the right acetabulum was not seen. Due to the fact that the acetabulum is very close to the bladder excessive activity from urine make it difficult to visualize the lesion. The possible solutions to overcome this problem include placement of urinary catheter or taking a postvoid view of the pelvis. False positive results have been reported in PET FDG imaging due to inflammatory processes (56,57), which could be a particular problem in lung cancer patients, where post obstructive pneumonia sometimes is confused

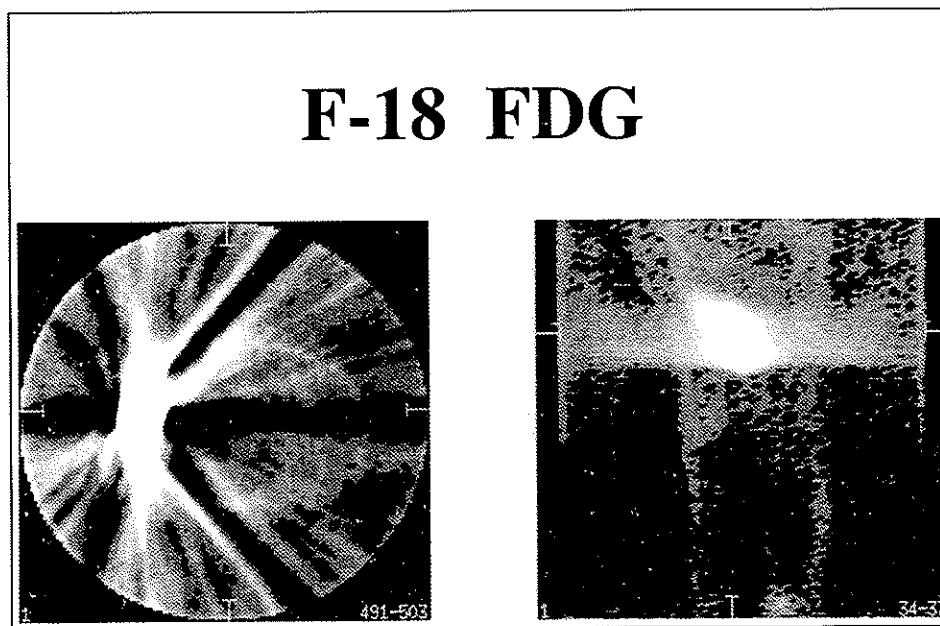


Fig. 10. Artifact created by reconstruction on transaxial (left) and sagittal (right) slices at the level of the bladder.

with tumor mass radiographically.

In conclusion, PET has great potential in the management of lung cancer, especially in the differentiation between benign and malignant lesions, the follow up of malignant lesions after therapy, and in the identification of recurrence as well as distant metastases.

Address Corresponded to: Abass Alavi MD, Division of Nuclear Medicine, Department of Radiology, Hospital of the University of Pennsylvania, 300 Spruce Street, Philadelphia, PA 19104, USA.

REFERENCES

1. Boring CC, Squires TS, Tong T. Cancer statistics. *CA Cancer J Clin* 43: 7-26; 1993.
2. Melamed MR, Flehinger BJ, Zaman MB, et al. Detection of true pathologic Stage I lung cancer in a screening program and the effect on survival. *Cancer* 47: 1182-1187; 1981.
3. Weiss W. The Philadelphia pulmonary neoplasm research project. *Appl Radiol* 8: 50-141; 1979.
4. Fontana RS. Screening for lung cancer. Recent experience in the United States. *Cancer Treat Res* 28: 91-111; 1986.
5. Eddy DM. Guidelines for the cancer-related checkup: Recommendations and rationale. *CA Cancer J Clin* 30:194-240; 1980.
6. Martini N, Burt ME, Bains MS, et al. Survival after resection of stage II non-small cell lung cancer. *Ann Thorac Surg* 54: 460-465; 1992.
7. Jensik RJ, Faber LP, Kittle CF. Sleeve lobectomy for bronchogenic carcinoma: the Rash-Presbyterian-St. Luke's medical center experience. *Int Surg* 71: 207-210; 1986.
8. Strauss GM, Langer MP, Elias AD, et al. Multimodality treatment of stage IIIA non-small cell lung carcinoma: A critical review of the literature and strategies for future research. *J Clin Oncol* 10: 829-838; 1992.
9. Niiranen A, Niitamo-Korhonen S, Kouri M, et al. Adjuvant chemotherapy after radical surgery for non-small cell lung cancer: A randomized study. *J Clin Oncol* 10: 1927-1932; 1992.
10. Belani CP. Multimodality management of regionally advanced non-small-cell lung cancer. *Semin Oncol* 20: 302-314; 1993.
11. McLoud TC, Bourgouin PM, Greenberg RW, et al. Bronchogenic carcinoma: Analysis of staging in the mediastinum with CT by correlative lymph node mapping and sampling. *Radiology* 182: 319-323; 1992.
12. Rhoads AC, Thomas JH, Hermreck AS, et al. Comparative studies of computerized tomography and mediastinoscopy for the staging of bronchogenic carcinoma. *Am J Surg* 152: 587-591; 1986.
13. Rendina EA, Bognolo DA, Mineo TC, et al. Computed tomography for the evaluation of intrathoracic invasion by lung cancer. *J Thorac Cardiovasc Surg* 94: 57-63; 1987.
14. Patterson GA, Ginsberg RJ, Poon PY, et al. A prospective evaluation of magnetic resonance imaging, computed tomography, and mediastinoscopy in the preoperative assessment of mediastinal node status in bronchogenic carcinoma. *J Thorac Cardiovasc Surg* 94: 679-684; 1987.
15. Osborne DR, Korobkin M, Ravin CE, et al. Comparison of plain radiography, conventional tomography, and computed tomography in detecting intrathoracic lymph node metastases from lung carcinoma. *Radiology* 142: 157-161; 1982.
16. Moak GD, Cockerill EM, Farber MO, et al. Computed tomography vs standard radiology in the evaluation of mediastinal adenopathy. *Chest* 82: 69-75; 1982.
17. McKenna RJ, Libshitz HI, Mountain CF, et al. Roentgenographic evaluation of mediastinal nodes for preoperative assessment in lung cancer. *Chest* 88: 206-210; 1985.
18. Mathews JJ, Richey HM, Helsel RA, et al. Thoracic computed tomography in the preoperative evaluation of primary bronchogenic carcinoma. *Arch Intern Med* 147: 449-453; 1987.
19. Glazer GM, Orringer MB, Gross BH, et al. The mediastinum in non-small cell lung cancer: CT surgical correlation. *Am J Roentgenol* 142: 1101-1105; 1984.
20. Ekholm S, Albrechtsoon U, Kugelberg J, et al. Computed tomography in preoperative staging of bronchogenic carcinoma. *J Comput Assist Tomogr* 4: 763-765; 1980.
21. Daly BD, Faling LJ, Bite G, et al. Mediastinal lymph node evaluation by computed tomography in lung cancer. *J Thorac Cardiovasc Surg* 94: 664-672; 1987.
22. Buy JN, Ghossain MA, Poirson F, et al. Computed tomography of mediastinal lymph nodes in nonsmall cell lung cancer: A new approach based on the lymphatic pathway of tumor spread. *J Comput Assist Tomogr* 12: 545-552; 1988.
23. Baron RL, Levitt RG, Sagel SS, et al. Computed tomography in the preoperative evaluation of bronchogenic carcinoma. *Radiology* 145: 727-732; 1982.
24. Staples CA, Muller NL, Miller RR, et al. Mediastinal nodes in bronchogenic carcinoma: Comparison between CT and mediastinoscopy. *Radiology* 167: 367-372; 1988.
25. Glazer GM, Orringer MB, Chenevert TL, et al. Mediastinal lymph nodes: Relaxation time/pathologic correlation and implications in staging of lung cancer with MR imaging. *Radiology* 168: 429-431; 1988.
26. Gefter WB. Magnetic resonance imaging in the evaluation of lung cancer. *Semin Roentgenol* 25: 73-84; 1990.
27. Pearlberg JL, Sandler MA, Beute GH, et al. Limitations of CT in evaluation of neoplasms involving chest wall. *J Comput Assist Tomogr* 11: 290-293; 1987.
28. Haggard AM, Pearlberg JL, Froelich JW, et al. Chest wall invasion by carcinoma of the lung: Detection by MR imaging. *Am J Roentgenol* 148: 1075-1078; 1987.
29. Webb WR, Gatsonis C, Zerhouni EA, et al. CT and MR imaging in staging non-small cell bronchogenic carcinoma: Report of the Radiology Diagnostic Oncology Group. *Radiology* 178: 705-713; 1991.

30. Heelan RT, Demas BE, Caravelli JF, et al. Superior sulcus tumors: CT and MR imaging. *Radiology* **170**: 637-641; 1989.
31. Oliver TW, Bernadino ME, Miller JJ, et al. Isolated adrenal masses in non-small-cell bronchogenic carcinoma. *Radiology* **153**: 217-218; 1984.
32. Berland LL, Koslin DB, Kenney PJ, et al. Differentiation between small benign and malignant adrenal masses with dynamic incremented CT. *Am J Roentgenol* **151**: 95-101; 1988.
33. Falk TH, te Strake L, Sandler MP, et al. Magnetic resonance imaging of the adrenal glands. *Radiographics* **7**: 343-370; 1987.
34. Reinig JW, Doppman JL, et al. Adrenal masses differentiated by MR. *Radiology* **158**: 81-84; 1968.
35. Glazer HS, Levitt RG, Lee JKT, et al. Differentiation of radiation fibrosis from recurrent pulmonary neoplasm by magnetic resonance imaging. *Am J Roentgenol* **143**: 729-730; 1984.
36. White CS, Templeton PA, Belani CP. Imaging in lung cancer. *Semin Oncol* **20**: 142-152; 1993.
37. Warburg O, Wind F, Negleis E. On the metabolism of tumors in the body, in Warburg O, ed: *The metabolism of tumors*. London: Constable; 1930: 254-270.
38. Monakhov NK, Neistadt EL, Shavlovskil MM, et al. Physicochemical properties and isoenzyme composition of hexokinase from normal and malignant human tissues. *J Natl Cancer Inst* **61**: 27-34; 1978.
39. Hatanaka M. Transport of sugar in tumor cell membranes. *Biochem Biophys Acta* **355**: 77-104; 1974.
40. Di Chiro G. Positron emission tomography using (F-18) fluorodeoxyglucose in brain tumors. *Invest Radiol* **22**: 360-371; 1987.
41. Di Chiro G, Brooks RA. PET-FDG of untreated and treated cerebral gliomas. *J Nucl Med* **29**: 421-422; 1988.
42. Kim CK, Alavi JB, Alavi A, et al. New grading system of cerebral gliomas using positron emission tomography with F-18 fluorodeoxyglucose. *J Neurooncol* **10**: 85-91; 1991.
43. Alavi JB, Alavi A, Chawluk J, et al. Positron emission tomography in patients with glioma: a predictor of prognosis. *Cancer* **62**: 1074-1078; 1988.
44. Strauss LG, Conti PS. The applications of PET in clinical oncology. *J Nucl Med* **32**: 623-648; 1991.
45. Gupta NC, Dewan NA, Phalen JJ, et al. Diagnostic efficacy of PET-FDG imaging in the differential diagnosis of a solitary pulmonary nodule. [Abstract] *Radiology* **181**: 152; 1991.
46. Kubota K, Matsuzawa T, Fujiwara T, et al. Differential diagnosis of lung tumor with positron emission tomography: A prospective study. *J Nucl Med* **31**: 1927-1932; 1990.
47. Knopp MV, Strauss LG, Bischoff, et al. PET imaging in the evaluation of recurrent thoracic tumors. [Abstract] *Radiology* **181**: 152; 1991.
48. Gupta NC, Boman BM, Frank AR, et al. Utility of PET-FDG imaging in treatment planning and monitoring of lung tumors. [Abstract] *Radiology* **181**: 152; 1991.
49. Whal RL, Cody RL, Hutchins GD, et al. Primary and metastatic breast carcinoma: Initial clinical evaluation with PET with the radiolabeled glucose analogue 2-deoxy-2(F-18) fluoro-D-glucose. *Radiology* **179**: 765-770; 1991.
50. Strauss LG, Clorius JH, Schlag P, et al. Recurrence of colorectal tumors: PET evaluation. *Radiology* **170**: 329-332; 1986.
51. Adler LP, Blair HF, Makley JT, et al. Correlation of FDG uptake with tumor grade in musculoskeletal tumors. [Abstract] *J Nucl Med* **31**: 756; 1990.
52. Griffeth LK, Dehdashti F, McGuire AH, et al. PET evaluation of soft tissue masses with F-18-fluorodeoxyglucose. *Radiology* **182**: 185-194; 1992.
53. Rege SD, Hoh CK, Glaspy JA, et al. Imaging of pulmonary mass lesions with whole-body positron emission tomography and fluorodeoxyglucose. *Cancer* **72**: 82-90; 1993.
54. Gupta NC, Frank AR, Dewan NA, et al. Solitary pulmonary nodules: Detection of malignancy with PET with 2-[F-18]-fluoro-2-deoxy-D-glucose. *Radiology* **184**: 441-444; 1992.
55. Choi Y, Brunken RC, Hawkins RA, et al. Determinants of myocardial glucose utilization assessed with dynamic FDG PET [abstract]. *Circulation* **84**: 11-425(1690); 1991.
56. Tahara T, Ichiya Y, Kuwabara Y, et al. High (F-18)-fluorodeoxyglucose uptake in abdominal abscesses: a PET study. *J Comput Assist Tomogr* **13**: 829-831; 1989.
57. Sasaki M, Ichiya Y, Kuwabara Y, et al. Ringlike uptake of (F-18) FDG in brain abscess: a PET study. *J Comput Assist Tomogr* **14**: 486-487; 1990.
58. Sasaki M, Ichiya Y, Kuwabara Y, et al. Fluorine-18-fluorodeoxyglucose positron emission tomography in technetium-99m-hydroxymethylenediphosphate negative bone tumors. *J Nucl Med* **34**: 288-290; 1993.
59. Adler L, Blair H, Makley J, et al. Noninvasive grading of musculoskeletal tumors using PET. *J Nucl Med* **32**: 1508-1512; 1991.